

## TRIBOLOGICAL BEHAVIORS OF DUPLEX DLC/Al<sub>2</sub>O<sub>3</sub> COATINGS FABRICATED USING MICRO-ARC OXIDATION AND FILTERED CATHODIC VACUUM ARC SYSTEM

X. L. WU<sup>\*,†</sup>, X. J. LI<sup>†</sup>, X. ZHANG<sup>\*</sup>, W. B. XUE<sup>\*</sup>, G. A. CHENG<sup>\*</sup> and A. D. LIU<sup>\*</sup>

*\*Key Laboratory of Beam Technology and Material Modification of Ministry of Education,  
Institute of Low Energy Nuclear Physics, Beijing Normal University Beijing 100875, P. R. China*

*†Department of Materials Science & Engineering, Beijing Normal University  
Beijing 100875, P. R. China  
‡wuxl@bnu.edu.cn*

Received 16 October 2006

Micro-arc oxidation technique (MAO) treatment produces a layer of alumina film on the surface of the aluminum alloy. A hard and uniform tetrahedral amorphous carbon film (diamond-like carbon, DLC) was deposited on the top of the alumina layer of the 2024 aluminum alloy by a pulsed filtered cathodic vacuum arc (FCVA) deposition system with a metal vapor vacuum arc (MEVVA) source. The morphology and tribological properties of the duplex DLC/Al<sub>2</sub>O<sub>3</sub> coating were investigated by a scanning electron microscope (SEM) and a ball-on-disk sliding tester. These results suggested that the duplex DLC/Al<sub>2</sub>O<sub>3</sub> coating had good adhesion and a low friction coefficient, which improved significantly the wear resistance of aluminum alloys.

*Keywords:* Aluminum alloy; micro-arc oxidation; DLC; FCVA; tribological behavior.

### 1. Introduction

Aluminum and its alloys are used to decrease the weight of mechanical parts in many fields.<sup>1,2</sup> In some situations, components made from aluminum alloys are often in tribological contact with different metals and media. However, poor wear resistance of the aluminum alloys limits their application. The surface modification technologies are proved to be an effective way to improve the tribological properties of aluminum alloys parts.<sup>3–7</sup> Anodizing is a popular technique for the surface modification of aluminum alloys. Nevertheless, anodized films of aluminum cannot meet the special application cases. A hard thick ceramic oxide coatings can be created on aluminum alloys by alternating-current micro-arc oxidation (MAO), which are initiated at potentials above the breakdown voltage of oxide films and move rapidly across the anodic surface.<sup>8–12</sup> The MAO alumina coating with high hardness can

improve the wear resistance of aluminum alloys. Good adhesion of the alumina layer to aluminum alloy substrates provides excellent load support for wear application.<sup>13–15</sup> However, the porous micro-structure of alumina coatings exhibits relatively high friction coefficients against many counter-face materials.<sup>16–19</sup>

In the last 10 years, much research has been carried out on hydrogen free diamond-like carbon (DLC) films which are also referred to as tetrahedral amorphous carbon (ta-C). DLC films are suitable as wear resistant coatings on cutting tools and automotive components, etc. due to their high hardness, low friction coefficients, and wear rates.<sup>20,21</sup> However, these applications often require the deposition of supporting inter-layers to provide the necessary adhesion and toughness, to optimize stress distribution and to allow operation in severe sliding/abrasive wear conditions.<sup>22–27</sup>

This research investigated the structure and tribological properties of the duplex DLC/Al<sub>2</sub>O<sub>3</sub> coating deposited on the surface of the aluminum alloy using a combined MAO and the pulsed filtered cathodic vacuum arc system technology that may significantly improve the tribological properties of the aluminum alloy.

## 2. Experimental Details

### 2.1. Coating preparation

Aluminum alloy (2024, AlCu4Mg1) disc samples with a diameter of 24 mm and a height of 7.88 mm were used for the experiments. The samples were polished up to 600<sup>#</sup> emery paper. A 30 kW alternating-current pulse power supply was employed to prepare alumina films on the sample surface. Sodium silicate electrolyte with additive was employed. The solution temperature was kept below 50°C, during the MAO treatment. The as-obtained coating has a thickness of 120 μm. Then the coatings were abraded to about 90 μm with a diamond disk and polished up to 1200<sup>#</sup> emery paper. A MEVVA ion implanter was used to perform the implantation of titanium ions at 40 keV. The implanted dose was  $5 \times 10^{16}$  ions/cm<sup>2</sup>. After the implantation, a layer of diamond-like carbon was deposited on the alumina layer with implanted titanium by the pulsed filtered cathodic vacuum arc system. The base pressure in the processing chamber was about  $2 \times 10^{-3}$  Pa. The cathodic arc source, a 100 mm diameter carbon plate of 99.99% purity, was used to produce plasma on the condition of 80 A direct current and 20 V voltage.

### 2.2. Tribological tests

A ball-on-disk tribo-meter (SRV, Optimal Co.) was used to evaluate wear resistance of the samples. The tribological tests were performed in dry air at ambient temperature. A 10 mm diameter ZrO<sub>2</sub> ball was used as the counter-face material. The wear volume loss of the films was determined from the wear grooves using a Talysurf 5P-120 (Rank Taylor Hobson Co., Holland) profile-meter.

### 2.3. Coating characterization

The surface morphology of films was investigated using a scanning electron microscope (SEM, S-4800,

Hitachi, JP). The composition profiles across the films were analyzed by the energy dispersive X-ray spectrum (EDX). X-ray diffraction (XRD) was performed using an X' PERT PRO MPD X-ray diffractometer to identify the phase constituents in the films. The Raman scattering spectra were acquired on the Jy-HR800 system with 7 mW semi-conductor laser at 532 nm.

## 3. Results and Discussion

### 3.1. Microstructure and phase composition

The X-ray diffraction pattern of the MAO coating is shown in Fig. 1. The MAO coating mainly consists of α-Al<sub>2</sub>O<sub>3</sub> and γ-Al<sub>2</sub>O<sub>3</sub>. The results of EDX of cross-sectional microstructure of the MAO coating also shows that about 90 μm MAO coating is a dense structure and combined well with the aluminum substrate (see Fig. 2a). Figure 2b shows a titanium element implanted in the subsurface and a carbon element deposited on the surface of the alumina oxide.

The Raman scattering spectrum of the surface of the DLC/Al<sub>2</sub>O<sub>3</sub> bilayer coating is shown in Fig. 3, which suggests a broad asymmetric Raman intensity distribution, which fitted to two Gaussian peaks, one “G” peak at 1580 cm<sup>-1</sup> and the other “D” peak at 1370 cm<sup>-1</sup>. The I<sub>D</sub>/I<sub>G</sub> ratio of the DLC/Al<sub>2</sub>O<sub>3</sub> bilayer coating is 0.11, which corresponds to a sp<sup>3</sup> content of approximately 89% in the coating. This

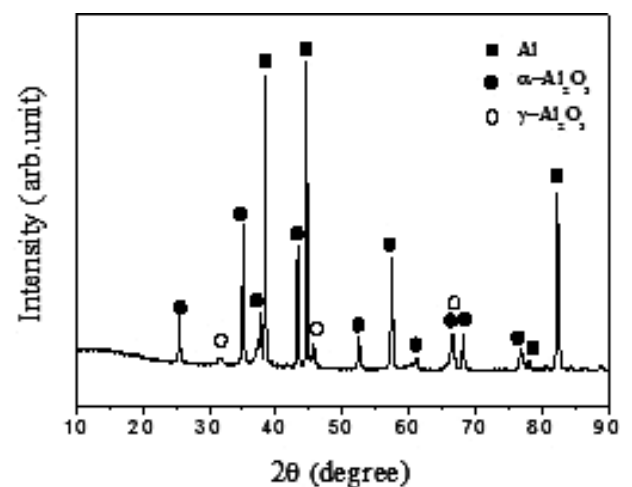
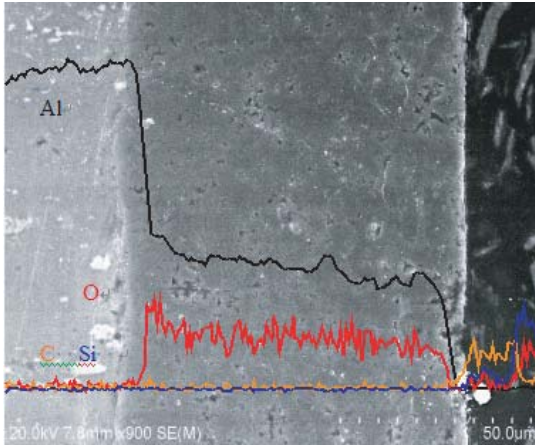
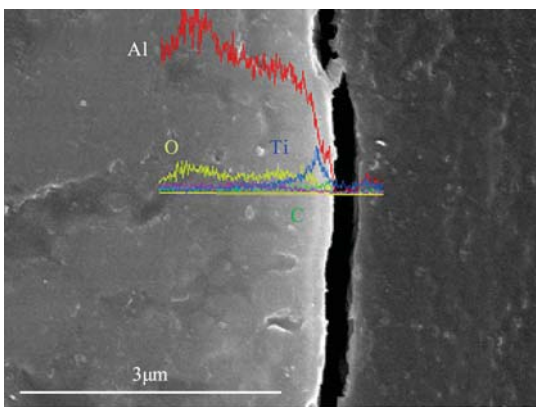


Fig. 1. X-ray diffraction spectrum of MAO coating of AlCu4Mg1 alloy.



(a)



(b)

Fig. 2. Cross-sectional microstructure (a) and the magnified image (b) of DLC/Al<sub>2</sub>O<sub>3</sub> film and XRD spectrum.

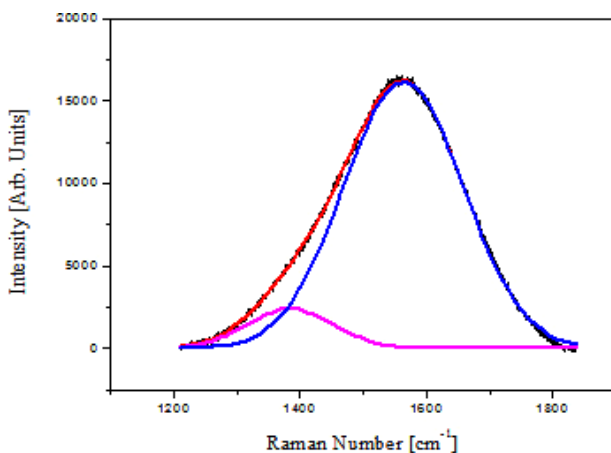


Fig. 3. Raman scattering spectrum of DLC/Al<sub>2</sub>O<sub>3</sub> coating on aluminum alloy.

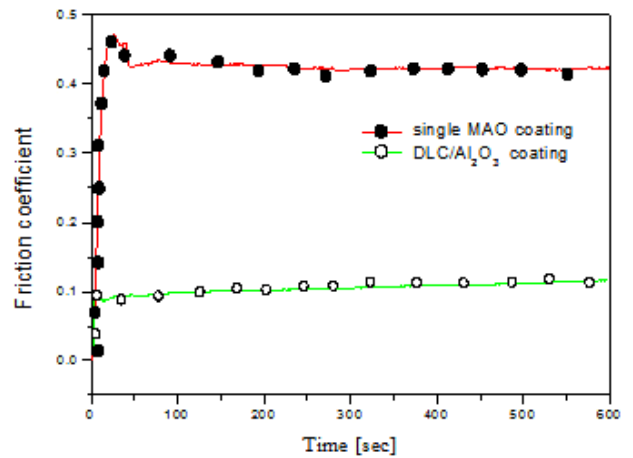


Fig. 4. Variation of friction coefficient of two films with wear time (load: 20 N, frequency: 20 Hz).

result suggests that the DLC/Al<sub>2</sub>O<sub>3</sub> coating is a ta-C film with high hardness and a low friction coefficient.

Friction coefficients of the DLC/Al<sub>2</sub>O<sub>3</sub> coating and the single MAO coating were examined, sliding under 20 and 50 N load, 12,000 laps, and dry air environment, as shown in Fig. 4. The friction coefficient for both films under the sliding conditions is steady after the first rise at the start. Furthermore, the friction coefficient for the DLC/Al<sub>2</sub>O<sub>3</sub> coating has a little decrease after many sliding cycles, which maybe is attributed to the lubrication effect of graphitization of the DLC film. The results demonstrate that the DLC/Al<sub>2</sub>O<sub>3</sub> coating has much lower a friction coefficient (about 0.1) than the single MAO coating (about 0.43).

The wear tracks of the samples were obtained (shown in Fig. 5) after sliding for 12,000 cycles against a zirconium dioxide ball, with an applied load 20 N in air at ambient temperature. The wear track of the single MAO coating is clearly visible (see Fig. 5a), while the wear track of DLC/Al<sub>2</sub>O<sub>3</sub> coatings is not clear (see Fig. 5b). The result illustrates that the DLC/Al<sub>2</sub>O<sub>3</sub> coating has much higher wear resistance under air environment owing to high hardness and low friction coefficient. A single MAO coating is characterized by abrasive wear and adhesive wear (see Fig. 5c), while the DLC/Al<sub>2</sub>O<sub>3</sub> coating is characterized by propagation of fatigue cracks formed beneath the surface (see Fig. 5d).<sup>26</sup>

The profiles of wear tracks of the DLC/Al<sub>2</sub>O<sub>3</sub> coating and the single MAO coating are shown in Fig. 6. The wear volume loss of the DLC/Al<sub>2</sub>O<sub>3</sub> coating ( $1.92 \times 10^{-4} \text{ mm}^3$ ) is much lower than that of

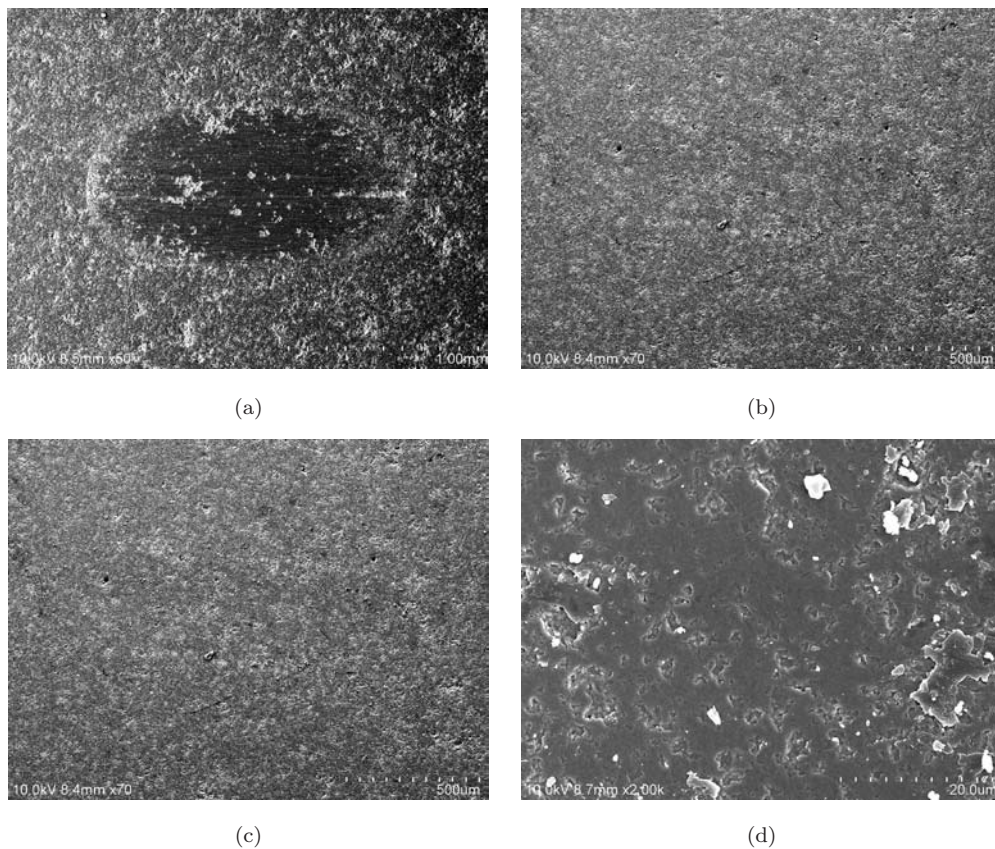


Fig. 5. Wear tracks of DLC/Al<sub>2</sub>O<sub>3</sub> and single MAO coating after 12,000 laps, under the applied load of (a) 20 N; (b) 50 N; (c) magnified image of (a); and (d) magnified image of (b), in air at ambient temperature.

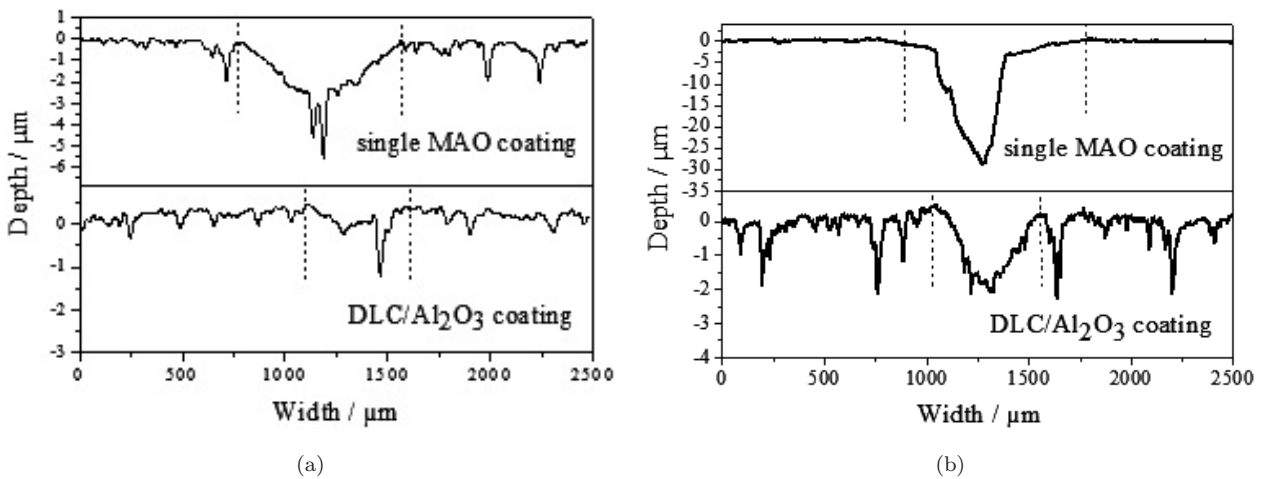


Fig. 6. Wear track micrograph of single layer MAO coating and DLC/Al<sub>2</sub>O<sub>3</sub> coating sliding at speed 1 cm/s, 12,000 laps, and (a) 20 N applied load; (b) 50 N applied load.

the single MAO coating ( $1.286 \times 10^{-3} \text{ mm}^3$ ) when applied 20 N load. As shown in Fig. 6b, when the applied load is increased to 50 N, the wear volume loss of the DLC/Al<sub>2</sub>O<sub>3</sub> coating ( $5.99 \times 10^{-4} \text{ mm}^3$ ) is

still much lower than that of the single MAO coating ( $7.541 \times 10^{-3} \text{ mm}^3$ ). This result suggests that the wear volume loss of both samples increases rapidly with the increase of the applied load. However, the

absolute wear volume loss of the DLC/Al<sub>2</sub>O<sub>3</sub> coating is much lower than that of the single MAO coating under 50 N applied loads compared with the absolute wear volume loss of the two samples under 20 N applied loads. The result indicates that the DLC/Al<sub>2</sub>O<sub>3</sub> coating can withstand the high load environments.

#### 4. Conclusion

Duplex DLC/Al<sub>2</sub>O<sub>3</sub> bilayer coatings are prepared on aluminum alloys using a combined MAO and pulsed filtered cathodic vacuum arc system technology. The fraction coefficient of DLC/Al<sub>2</sub>O<sub>3</sub> is much lower than that of the single MAO coating. The tribological property of a single MAO coating for aluminum alloys was improved much by the DLC/Al<sub>2</sub>O<sub>3</sub> coating.

#### Acknowledgments

This project was sponsored by SRF for ROCS, SEM and supported by Mengya foundation of Beijing Academy of Science and Technology.

#### References

1. E. A. Starke Jr. and J. T. Staley, *Prog. Aerospace Sci.* **32** (1996) 131.
2. W. S. Miller, L. Zhuang, J. Bottema, A. J. Wittebrood, P. De Smet, A. Haszler and A. Vieregge, *Mater. Sci. Eng. A* **280** (2000) 37–39.
3. J. Sun, L. Weng and Q. Xue, *Vacuum* **62** (2001) 337.
4. Z. Zhan, X. Ma, L. Feng, Y. Sun and L. Xia, *Wear* **220** (1998) 161.
5. E. Lugsheider, G. Krämer, C. Barimani and H. Zimmermann, *Surf. Coat. Technol.* **74–75** (1995) 497.
6. T. Bell, K. Mao and Y. Sun, *Surf. Coat. Technol.* **108–109** (1998) 360.
7. J. C. Szcancoski, C. E. Foerster, F. C. Serbena, T. Fitz, U. Kreißig, E. Richter, W. Möller, C. M. Lepienski, P. C. Soares Jr. and C. J. de M. Siqueira, *Surf. Coat. Technol.* **201** (2006) 1488.
8. W. Xue, Z. Deng, R. Chen and Z. Zhang, *Surf. Eng.* **16** (2000) 344.
9. W. Xue, Z. Deng, R. Chen and Z. Zhang, *Thin Solid Films* **372** (2000) 114.
10. A. L. Yeroklin, X. Nie, A. Leyland, A. Matthews and S. J. Dowey, *Surf. Coat. Technol.* **122** (1999) 73.
11. C. Chen, Q. Dong and D. Wang, *Surf. Rev. Lett.* **12** (2005) 781.
12. C. Chen, Q. Dong and D. Wang, *Surf. Rev. Lett.* **13** (2006) 63.
13. W. Xue, C. Wang, Z. Deng, R. Chen, Y. Li and Z. Zhang, *J. Phys. Condens. Matter* **14** (2002) 10947.
14. W. Xue, C. Wang, Y. Li, R. Chen and Z. Zhang, *ISIJ Int.* **42** (2002) 1273.
15. A. L. Yeroklin, A. Shatrov, V. Samsonov, P. Shashkov, A. Leyland and A. Matthews, *Surf. Coat. Technol.* **199** (2005) 150.
16. X. Nie, E. I. Meletis, J. C. Jiang, A. Leyland, A. L. Yeroklin and A. Matthews, *Surf. Coat. Technol.* **149** (2002) 245.
17. P. A. Dearnley, J. Gummersbach, H. Weiss, A. A. Ogwu and T. J. Davies, *Wear* **225–259** (1999) 127.
18. W. Xue, Z. Deng, R. Chen, Z. Zhang and H. Ma, *J. Mater. Sci.* **36** (2001) 2615.
19. W. Xue, J. Du, X. Wu and Y. Lai, *ISIJ Int.* **46** (2006) 287.
20. P. J. Martin and A. Bendavid, *Thin Solid Films* **394** (2001) 1.
21. X. Zhang, Z. Yi, T. Zhang, X. Wu, G. Wang and H. Zhang, *Surf. Coat. Technol.* **161** (2002) 120.
22. E. I. Meletis, A. Erdemir and G. R. Fenske, *Surf. Coat. Technol.* **73** (1995) 39.
23. A. A. Voevodin, J. M. Schneider, C. Rebholz and A. Matthews, *Tribol. Int.* **29** (1996) 559.
24. X. Nie, A. Wilson, A. Leyland and A. Matthews, *Surf. Coat. Technol.* **121** (2000) 50.
25. E. Dekempeneer, K. Van Acker, K. Vercammen, J. Meneve, D. Neerincx, S. Eufinger, W. Pappaert, M. Sercu and J. Smeets, *Surf. Coat. Technol.* **142–144** (2001) 669.
26. X. Yu, X. Zhang, C. Wang, M. Hua and L. Wang, *Vacuum* **75** (2004) 231.
27. W. Zhang, A. Tanaka, B. S. Xu and Y. Koga, *Diamond Relat. Mater.* **14** (2005) 1361.